Hydrogen Exchange Kinetics in a Membrane Protein Determined by ^{15}N NMR Spectroscopy: Use of the INEPT Experiment To Follow Individual Amides in Detergent-Solubilized M13 Coat Protein†

Gillian D. Henry and Brian D. Sykes*

MRC Group in Protein Structure and Function and Department of Biochemistry, University of Alberta, Edmonton, Alberta T6G 2H7, Canada

Received January 10, 1990; Revised Manuscript Received March 12, 1990

ABSTRACT: The coat protein of the filamentous coliphage M13 is a 50-residue polypeptide which spans the inner membrane of the *Escherichia coli* host upon infection. Amide hydrogen exchange kinetics have been used to probe the structure and dynamics of M13 coat protein which has been solubilized in sodium dodecyl sulfate (SDS) micelles. In a previous ^1H nuclear magnetic resonance (NMR) study [O'Neil, J. D. J., & Sykes, B. D. (1988) *Biochemistry 27*, 2753–2762], multiple exponential analysis of the unresolved amide proton envelope revealed the existence of two slow "kinetic sets" containing a total of about 30 protons. The slower set (15–20 amides) originates from the hydrophobic membrane-spanning region and exchanges at least 10^5-fold slower than the unstructured, non-H-bonded model polypeptide poly(DL-alanine). Herein we use ^{15}N NMR spectroscopy of biosynthetically labeled coat protein to follow individual, assigned, slowly exchanging amides in or near the hydrophobic segment. The INEPT (insensitive nucleus enhancement by polarization transfer) experiment [Morris, G. A., & Freeman, R. (1979) *J. Am. Chem. Soc. 101*, 760–762] can be used to transfer magnetization to the ^{15}N nucleus from a coupled proton; when ^{15}N-labeled protonated protein is dissolved in ^2H_2O, the INEPT signal disappears with time as the amide protons are replaced by solvent deuterons. Amide hydrogen exchange is catalyzed by both H^+ and OH^- ions. Base catalysis is significantly more effective, resulting in a characteristic minimum rate in model peptides at pH $\cong$3. Rate versus pH profiles have been obtained by using the INEPT experiment for the amides of leucine-14, leucine-41, tyrosine-21, tyrosine-24, and valines-29, -30, -31, and -33 in M13 coat protein. The valine residues exchange most slowly and at very similar rates, showing an apparent 10^6-fold retardation over poly(DL-alanine). A substantial basic shift in the pH of the minimum rate (up to 1.5 pH units) was also observed for some residues. Possible reasons for the shift include accumulation of catalytic H^+ ions at the negatively charged micelle surface or destabilization of the negatively charged transition state of the base-catalyzed reaction by either charge or hydrophobic effects within the micelle. The time-dependent exchange-out experiment is suitable for slow exchange rates (k_{ex}), i.e., less than (1–2) $\times$ 10^{-4} s^{-1}. The INEPT experiment was also adapted to measure some of the more rapidly exchanging amides in the coat protein (leucine-14 at higher pH values and glycine-3) using either saturation transfer from water ($k_{ex} \cong 1/T_{1,amide} \cong 2$ s^{-1}) or exchange effects on the polarization transfer step itself ($k_{ex} \cong J_{NH} \cong 100$ s^{-1}, where J_{NH} is the ^{15}N–^1H coupling constant). Retardations of individual rates with respect to poly(DL-alanine) are analyzed in terms of the local unfolding model for amide exchange. The results of all of these experiments are consistent with previous models of the coat protein in which a stable segment extends from the hydrophobic membrane-spanning region through to the C-terminus, whereas the N-terminal region is undergoing more extensive dynamic fluctuations.

Conformational fluctuations in proteins play an important part in their activities and interactions with other molecules. Historically, amide hydrogen exchange kinetics provided some of the initial insights into the dynamic aspects of protein structure (Linderstrom-Lang, 1955; Linderstrom-Lang & Schellman, 1957), and amide exchange continues to be one of the more important experimental approaches. Although the precise nature of the structural fluctuations which give rise to exchange is in dispute (Woodward et al., 1982; Barksdale & Rosenberg, 1982; Englander & Kallenbach, 1984), it is generally agreed that amides which are hydrogen bonded exchange considerably more slowly than those which are not. More importantly, H-bond breakage is required for exchange to occur; thus, hydrogen exchange kinetics can serve as a sensitive probe of the dynamic events which give rise to the severing of H bonds. Clearly the exchange rates of individual amide protons are most useful, and recently, ^1H nuclear magnetic resonance (NMR)[1] spectroscopy has been used to provide the resolution required to determine individual rates in a number of small proteins. The basic pancreatic trypsin inhibitor has been studied intensively under a wide variety of conditions (e.g., Richarz et al., 1979; Wuthrich & Wagner, 1979; Wagner, 1983; Roder et al., 1985a,b; Tuchsen & Woodward, 1985a,b) and remains the most thoroughly in-

† Supported by the Medical Research Council of Canada (MRC Group in Protein Structure and Function).

* Address correspondence to this author at the Department of Biochemistry, University of Alberta.

[1] Abbreviations: DEPT, distortionless enhancement by polarization transfer; INEPT, insensitive nucleus enhancement by polarization transfer; J_{NH}, ^{15}N–^1H coupling constant; K_{D_2O}, ionic product of D_2O; K_w, ionic product of water; NMR, nuclear magnetic resonance; NOE, nuclear Overhauser effect; pH*, pH meter reading in ^2H_2O; pH_{min}, pH of minimum exchange rate; ppm, parts per million; SDS, sodium dodecyl sulfate; T_1, spin–lattice relaxation time; T_2, spin–spin relaxation time, τ_c, overall rotational correlation time; γ_H, gyromagnetic ratio of ^1H; γ_N, gyromagnetic ratio of ^{15}N.

0006-2960/90/0429-6303$02.50/0

```
                    5                   10
ALA GLU GLY ASP ASP PRO ALA LYS ALA ALA

                   15                  20
PHE ASN SER LEU GLN ALA SER ALA THR GLU

                   25                  30
TYR ILE GLY TYR ALA TRP ALA MET VAL VAL

                   35                  40
VAL ILE VAL GLY ALA THR ILE GLY ILE LYS

                   45                  50
LEU PHE LYS LYS PHE THR SER LYS ALA SER
```

FIGURE 1: Sequence of M13 coat protein (van Wezenbeek et al., 1980). Labeled residues that are discussed in the text are highlighted.

vestigated example of hydrogen exchange behavior in a protein. In addition, virtually complete amide exchange profiles (i.e., exchange rate as a function of sequence) are available for bull seminal inhibitor IIA (Wüthrich et al., 1984), apamin (Dempsey, 1986), the lac repressor headpiece (Boelens et al., 1985), and the α-amylase inhibitor Tendamistat (Qiwen et al., 1987). Sequential exchange rates in helical regions of cytochrome *c* (Wand et al., 1986), ribonuclease S (Kuwajima & Baldwin, 1983), and myoglobin (Vasent Kumar & Kallenbach, 1985) have also been measured. We are using amide hydrogen exchange kinetics to explore the conformational fluctuations which occur in the backbone of M13 coat protein, a small integral membrane protein derived from a filamentous phage. It is anticipated that hydrogen exchange rates will allow us to locate regions of stable secondary structure and shed light on the dynamic events which give rise to exchange.

The filamentous coliphage M13 is a member of a family of related bacterial viruses, all of which are nonlytic and composed essentially of a single-stranded DNA circle together with many copies of a major coat protein. Several minor capsid proteins are also present in very low amounts. Although the phage particle contains no lipid, the coat protein is inserted as an integral protein in the inner membrane of the *Escherichia coli* host upon infection [see Wickner (1988) for a recent review]. The sequence of M13 coat protein (Figure 1)[2] reflects its ability to span the lipid bilayer, a 19-residue highly hydrophobic central core is flanked by hydrophilic N- and C-terminal regions. Upon removal from the phage, the protein aggregates extensively in the absence of solubilizing amphiphiles (Cavalieri et al., 1976; Noxaki et al., 1978). The three-dimensional structure of the detergent- or lipid-bound form is not known, but various structural and dynamic aspects of M13 coat protein (and the equivalent protein in the related phage Pf1) have been probed spectroscopically (e.g., Nozaki et al., 1976; Hagen et al., 1979; Cross & Opella, 1979; Foder et al., 1980; Dettman et al., 1984; Wilson & Dahlquist, 1985; Datema et al., 1987; Leo et al., 1987; Bogusky et al., 1988). A number of different models have been proposed on the basis of these data (e.g., Webster & Cashman, 1979; Fodor et al., 1980; Henry & Sykes, 1990a). The micelle-bound protein is believed to be a dimer (Makino et al., 1975; Cavalieri et al., 1976; Henry & Sykes, 1990b).

Previously we have used ^{13}C NMR relaxation parameters to monitor the dynamics of the protein backbone for sodium deoxycholate and sodium dodecyl sulfate (SDS) solubilized coat protein. These experiments are sensitive to motions which occur on a time scale faster than the overall correlation time of the complex, τ_c, which is about 10 ns (Henry et al., 1986, 1987a). It was concluded that such motions occur with significant amplitude only at the extreme ends of the polypeptide chain, perhaps four residues from each of the N- and C-termini. Experiments which exploit the negative nuclear Overhauser effect (NOE), which is observed for ^{15}N nuclei undergoing high-frequency motions, reach essentially the same conclusions (Bogusky et al., 1985, 1988; Shiksnis et al., 1987). Amide hydrogen exchange kinetics provide a probe of events which may take place on a much slower time scale.

Amide exchange in proteins is generally measured by following the intensity of the amide proton signal (observed by ^1H NMR) as a function of time after protonated protein is dissolved in deuterated solvent. For larger proteins or the detergent-solubilized coat protein (which has an apparent relative molecular mass of 27 000; Makino et al., 1975), individual amides may not be resolved, even by two-dimensional NMR. Nevertheless, multiple exponential analysis of the decay of the amide proton envelope in SDS-solubilized coat protein has been used to show that the amides fall into distinct kinetic sets. The slowest set, which arises from the hydrophobic core of the protein, exchanges about 10^5-fold more slowly than the unstructured model peptide poly(DL-alanine) (O'Neil & Sykes, 1988). In order to follow individual amides in the coat protein, we have resorted to isotope-directed methods. Resolution is provided by the isotopic label which is incorporated biosynthetically; this also simplifies the assignment problem (Henry et al., 1987a). Previous experiments (Henry et al., 1987b) employed a carbonyl carbon equilibrium isotope shift technique to measure relatively rapid exchange rates in the protein ($<10^4$-fold retardation). Herein we describe a second isotope-directed technique using ^{15}N-labeled coat protein which allows access to individual slowly exchanging amides of the hydrophobic core. In addition, the ^{15}N experiment, which involves polarization transfer from the attached amide proton to the ^{15}N nucleus, can be adapted to measure moderately fast rates through saturation transfer from water and more rapid rates through interference with the polarization transfer and subsequent refocusing steps (Leighton & Lu, 1987).

Experimental Procedures

Materials

Auxotrophic *Escherichia coli* strains G11a1 (CGSC 5168, Hfr, *rel* A1, *ilv* 229, *met* B1, *amp* A1), AT2457 (CGSC 4507, Hfr, *thi* 1, *gly* A6, *rel* A1, λ−, *spo* T1), and AT2471 (CGSC 4510 Hfr, *thi* 1, *tyr* Ay, *rel* 1, λ−) were obtained from Barbara Bachmann, *E. coli* Genetic Stock Centre, Yale University School of Medicine. L-[^{15}N]Leucine, DL-[^{15}N]valine, DL-[^{15}N]tyrosine, [^{15}N]glycine, and [1-^{13}C]glycine (all 99 atom %) were purchased from MSD Isotopes (Pointe Claire, Dorval, Quebec). Sodium dodecyl sulfate (electrophoretic grade) was obtained from ICN Biomedicals Canada (Montreal, Quebec).

Methods

Growth of Labeled Phage. M13 phage was labeled with ^{15}N as described by Henry et al. (1986) with the following modifications: a 0.05 g L^{-1} aliquot of the appropriate labeled L-amino acid was included in the culture medium together with 0.1 g L^{-1} each of the other 19 amino acids to suppress cellular transaminases (Cross & Opella, 1985); 0.1 g L^{-1} each of adenine and guanosine (guanine is insoluble in the growth medium) and 0.05 g L^{-1} each of thymine, cytosine, and uracil were also added to suppress purine and pyrimidine biosynthesis, respectively. Auxotrophic strains of *E. coli* (G11a1 for valine and leucine, AT2471 for tyrosine, and AT2457 for glycine) were used. Under these conditions, the isotopic label was not

[2] Previous publications from this laboratory included an error in the protein sequence [see O'Neil and Sykes (1989) and preceding papers]. Residue 12 is known to be asparagine in M13 (van Wezenbeek et al., 1980) and not aspartic acid which is found in the otherwise identical proteins from the closely related phages f1 and fd (Asbeck et al., 1969; Nakashima & Konigsberg, 1974).

incorporated into other amino acid residues at a detectable level.

Preparation of Samples for Amide Exchange. SDS-solubilized coat protein was prepared as described by Henry et al. (1986). The phage DNA was removed by gel filtration on Sephacryl S-200 SF (Woolford & Webster, 1975) equilibrated in 5 mM sodium borate, pH 9.0, 90 mM sodium chloride, and 10 mM SDS. Protein-containing fractions were pooled and concentrated to 4 mL by ultrafiltration; the pH was adjusted to 7.5, and the sample was freeze-dried. The freeze-drying process does not affect the exchange rates (O'Neil & Sykes, 1988). Amide exchange was initiated by dissolving the sample in 4 mL of lightly buffered ^2H_2O solution at an appropriate pH*. Sodium formate, glycine, sodium succinate, sodium acetate, and sodium phosphate were used as buffers, and the pH* was adjusted further if necessary by addition of small amounts of concentrated acid or base. Final pH* values were taken at the end of each experiment. Each sample of protein was prepared identically to avoid possible variations in the quantity of bound detergent. The protein concentration was about 2.5 mM, determined by the absorbance at 280 nm using a molar absorptivity of 8290 M^{-1} cm^{-1}. Amide exchange measurements in water were performed by direct addition of 0.4 mL of ^2H_2O buffer (to provide a lock signal) to 3.6 mL of concentrated protein. pH* values are direct meter readings, uncorrected for deuterium isotope effects.

NMR Spectroscopy. ^{15}N spectra were recorded at 30.4 MHz on a Nicolet NT 300 WB NMR spectrometer equipped with a 12-mm ^{15}N probe. The 90° pulse length was 45 μs. Decoupled INEPT spectra were acquired by using the refocused INEPT pulse sequence (Morris, 1980) with broad-band proton decoupling during the acquisition period. The acquisition time and the delay between transients were both 1 s. J_{NH} was taken to be 94.5 Hz (the value measured for N-acetylglycine) throughout. ^{15}N chemical shifts are reported relative to 1 M $^{15}NH_4Cl$ in 2 M HCl at 0 ppm (external standard). The slow rates of amide exchange in M13 coat protein (especially at low pH values) required periodic acquisition of spectra, sometimes over many months. It was thus necessary to monitor and correct for instrumental instabilities which occurred during this period. The INEPT experiment is sensitive to inaccuracies in the proton pulse lengths (Morris, 1984); therefore, the decoupler coil was tuned, and the 90° pulse length was calibrated before each set of ^{15}N experiments. As amide exchange rates were determined from a time course which extended over weeks or months, spectra that were not collected continuously (i.e., during a single period of instrument time) were normalized according to the integrated intensity of a standard sample containing 10 mM [^{15}N]acetylglycine, 90 mM sodium chloride, 5 mM sodium borate, and 10 mM SDS in 10% ^2H_2O, pH 4.0. Variations in the intensity of this sample were usually within ±10%, but deviations of as much as 20% occurred occasionally. Samples were maintained at room temperature, which remained constant at 23 °C throughout the time course of exchange. Spectra were also recorded at a probe temperature of 23 °C. Very little sample heating occurred during acquisition; a temperature of 24 °C was measured on a test sample immediately after acquisition of a typical INEPT dataset.

Calculation of Exchange Parameters. K_w values of 14.92 (^2H_2O) and 14.06 (^1H_2O) were calculated from the data of Covington et al. (1966) and used throughout. Problems arise when comparing rates measured in ^2H_2O (direct exchange-out) with those measured in ^1H_2O (saturation and polarization transfer) due to a kinetic isotope effect of unknown magnitude and the correct determination of the $^2H^+$ ion concentration in ^2H_2O using the glass electrode [see Glasoe and Long (1960)]. Both these effects are conveniently eliminated by comparing experimental values with values determined for poly(DL-alanine) under similar conditions. Reliable values of k_D and k_{OD} (actually rate constants for the exchange of ^1H by ^2H) were determined by Englander et al. (1979) for poly(DL-alanine) at 20 °C. By use of activation enthalpies given therein, and accounting for the effect of the activation enthalpy of ^2H_2O ionization on the base-catalyzed rate [see Roder et al. (1985b)], values of $k_D = 0.421$ M^{-1} s^{-1} and $k_{OD} = 2.97 \times 10^8$ M^{-1} s^{-1} were calculated at 23 °C. Unfortunately, k_H and k_{OH} values (i.e., rate constants for the exchange of ^1H by ^1H) for poly(DL-alanine) are not available; however, Molday et al. (1972) measured both k_D and k_{OD} for exchange-out in ^2H_2O and k_H and k_{OH} from line-shape analysis in ^1H_2O for a number of small peptides. Taking the rate constants calculated for *N*-acetylalanine methylamide (adjusted to 23 °C), a k_{OH} value of 3.43×10^7 M^{-1} s^{-1} was calculated for poly(DL-alanine) in ^1H_2O. Experimental k_{OH} and k_{OD} values were also corrected (when stated) for primary sequence effects by using the model peptide data of Molday et al. (1972).

THEORY

Amide Hydrogen Exchange. Hydrogen exchange in model, non-H-bonded peptides such as poly(DL-alanine) is catalyzed by H^+ and OH^- and is generally described

$$k_{ex} = k_H[H^+] + k_{OH}[OH^-] \quad (1)$$

where k_{ex} is the pseudo-first-order rate constant for exchange and k_H and k_{OH} are acid- and base-catalyzed rate constants (Englander & Kallenbach, 1984), respectively. General acid or base catalysis is negligible at room temperature (Englander et al., 1979), and catalysis by buffer ions does not occur for peptide amides (Englander & Kallenbach, 1984). OH^- ions are many times more effective than H^+, resulting in a characteristic minimum exchange rate of 3.0 for poly(DL-alanine). Above pH 4 the rate increases 10-fold for each unit rise in pH. In proteins, structural features retard the exchange rate, resulting in a downward shift of the rate vs pH curve. An expression for the pH of minimum rate (pH_{min}) can be derived from eq 1 (Leichtling & Klotz, 1966):

$$pH_{min} = \tfrac{1}{2}pK_w - \tfrac{1}{2}\log(k_{OH}/k_H) \quad (2)$$

Measurement of H Exchange Rates. The INEPT experiment (insensitive nucleus enhancement by polarization transfer) was introduced as a method for increasing the sensitivity of nuclei of low gyromagnetic ratio (γ) (Morris & Freeman, 1979; Morris, 1980). For a two-spin system such as ^{15}N–H, this is achieved by transferring the population difference which exists across the two proton transitions to the nitrogen transitions. Under optimal conditions, the sensitivity is enhanced by $|\gamma_H/\gamma_N|$, i.e., 10-fold, although other processes also contribute (Morris, 1984). This is clearly advantageous in proteins where sensitivity is always at a premium. The polarization transfer experiment will not work, however, if the amide proton is replaced by a solvent deuteron or if it exchanges too rapidly with solvent protons for magnetization transfer to take place. Both of these properties may be exploited in order to measure the exchange rates of labile protons. A third type of experiment, based on transfer of saturation from water, has also been devised.

Slow Exchange Rates. Of the above methods, the first is a time-dependent "exchange-out" experiment suitable for slowly exchanging amides. When ^{15}N-labeled protonated

protein is dissolved in buffered ^2H_2O, the intensity of the ^{15}N INEPT signal decays exponentially with time, and the rate constant k_{ex} can be obtained at different pH values in a series of different experiments.

Intermediate Exchange Rates. Two further exchange regimes can be monitored if the experiment is performed in water rather than ^2H_2O. In polarization transfer pulse sequences, the optimal delay between transients is governed by the amide proton T_1, that is, recovery of the equilibrium population differences across the proton transitions following saturation during ^1H decoupling in the acquisition model. Typically a compromise is reached between the complete recovery of signal (which is exponential) and the number of transients which can be acquired in a given time. If k_{ex} is of the order of $1/T_{1,amide}$, then at moderate recycle delays the INEPT signal is diminished due to transfer of saturation from the more slowly recovering water protons. Unlike conventional homonuclear saturation transfer (e.g., O'Neil & Sykes, 1988), both the amide proton and water are saturated during proton decoupling. The following equation for the intensity (I) can be derived according to Forsen and Hoffman (1963):

$$I = I_0 + C_1 \exp[(T_{1,amide}^{-1} + k_{ex})t] + C_2 \exp(t/T_{1,water}) \quad (3)$$

where C_1 and C_2 are constants [defined by Forsen and Hoffman (1963), case IV] and t is the relaxation delay. In contrast to direct exchange-out techniques, this is an "equilibrium" method; the exchange rate is determined from the intensity of the signal which can be varied according to pH in a single experiment (see below). Amide proton T_1 values in the coat protein are on the order of 0.5 s, corresponding to appropriate k_{ex} values of about 2 s^{-1}. This experiment will be discussed in more detail elsewhere (Henry and Sykes, unpublished results).

Fast Exchange Rates. A second critical period for amide exchange occurs in the INEPT experiment when the components of the ^{15}N doublet are brought into antiphase along the x axis of the rotating frame prior to the polarization transfer pulse and subsequent refocusing before application of the decoupler pulse. If the lifetime of the amide is of this order ($1/J_{NH} \cong 0.01$ s, where J_{NH} is the ^{15}N–H coupling constant), then the relevant phase information is lost, and the intensity of the signal is reduced (Leighton & Lu, 1987). In the base-catalyzed regime, the intensity is given:

$$I = I_0 \exp(-k_{OH}[OH^-]/J_{NH}) \quad (4)$$

In order to measure exchange rates of the order of J in this way, care must be taken to ensure that the delay between transients is significantly longer than the apparent T_1 value. Alternatively, single-frequency decoupling avoids saturation of the water altogether, but may be applicable to a limited number of amides within a given sample. The exchange rates which can be determined by using either the polarization transfer or the saturation transfer experiments are of a similar order to those obtained from the collapse of ^{15}N–H coupling with pH observed by direct ^{15}N detection (Blomberg & Rüterjans, 1978). Both the sensitivity and the resolution are much improved in the INEPT experiment, however.

Results

Resonance Assignments of ^{15}N-Labeled Coat Protein in SDS Micelles. Much structural work has been performed on M13 coat protein solubilized in dodecyl sulfate micelles as it is extremely stable in this form over a wide range of pH values (e.g., Cross & Opella, 1979; Bogusky et al., 1985, 1988; Henry et al., 1987a,b; O'Neil & Sykes, 1988). Nevertheless, the overall structure of the protein appears to be reasonably similar in other detergents such as deoxycholate (Nozaki et al., 1978; Henry et al., 1986; Henry & Sykes, 1990a). Representative INEPT spectra of [^{15}N]leucine, valine, tyrosine, and glycine-labeled coat protein in SDS micelles are shown in Figure 2; these spectra were acquired in ^1H_2O (10% ^2H_2O) buffer at low pH values to minimize amide hydrogen exchange rates. Excluding the effects of exchange, all of the spectra in Figure 2 are remarkably insensitive to pH, suggesting that no major conformational changes occur over the pH range of this study. With the exception of glycine-3 and leucine-14, all of the labeled residues are found in the vicinity of the hydrophobic segment and might be expected to be among those most closely associated with the detergent molecules.

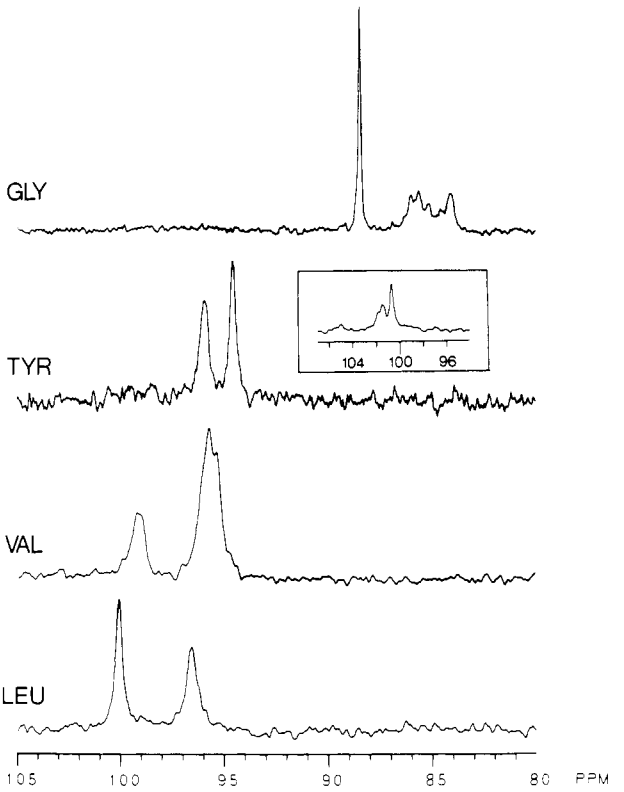

FIGURE 2: Proton-decoupled INEPT spectra of ^{15}N-labeled coat protein in SDS micelles and ^1H_2O buffer (10% ^2H_2O), pH 4–6, 23 °C, 5000 transients. The inset shows [1-^{13}C]glycine/[^{15}N]tyrosine double-labeled protein at 40 °C; carbon–nitrogen coupling reveals the downfield peak to belong to tyrosine-21.

The two leucine residues (Figure 2) are well resolved and can be assigned on the basis of their amide exchange rates. Leucine-41 amide has been shown previously by ^{13}C NMR to be retarded at least 10^4-fold over poly(DL)alanine (Henry et al., 1987b); therefore, the more rapidly exchanging downfield resonance must belong to leucine-14. By contrast, only one of the four valine ^{15}N resonances (designated valine-A) is completely resolved, the other three giving rise to a complex peak (valine-B) due to extensive resonance overlap (Figure 2). The individual peaks can be discerned to some extent by using resolution enhancement techniques; however, experiments performed at higher fields show that the [^{15}N]valine spectrum is actually quite complex (Henry & Sykes, 1990b). Since the exchange rates of the three overlapping residues are about the same, no attempt was made to resolve or assign them. The valine residues occur in the sequence Val-Val-Val-Ile-Val within the hydrophobic core of the protein, and it is quite possible that they share a similar environment. Both tyrosine residues (tyrosine-21 and tyrosine-24) occur at the N-terminal end of the hydrophobic segment. They were as-

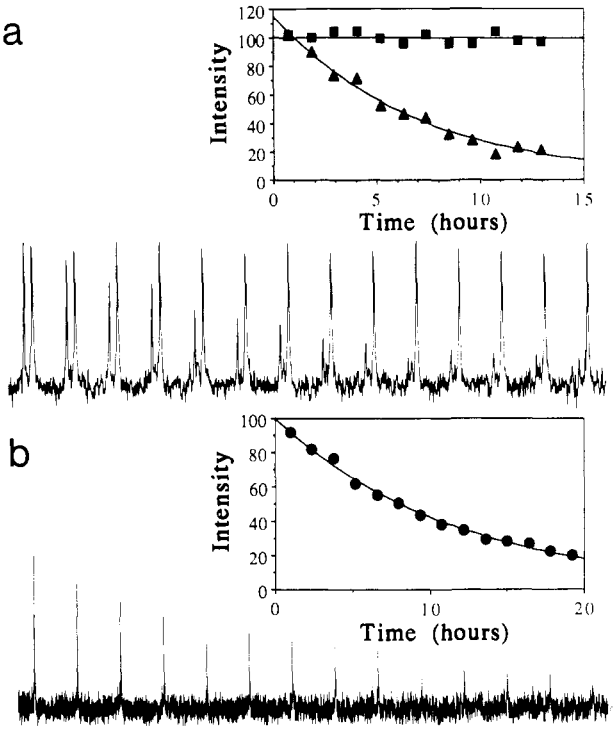

FIGURE 3: Time-dependent decay of the INEPT ^{15}N NMR resonances of [^{15}N]leucine-labeled coat protein; exchange was initiated by dissolving protonated protein in ^2H_2O at time zero. (a) Exchange at pH* 3.5, 2000 transients (1.11 h per time point). The decay of leucine-14 is first order [inset (▲)], k_{ex} = (3.93 ± 0.19) × 10^{-5} s^{-1}. The intensity of leucine-41 (■) does not appear to change on this time scale. (b) Exchange at pH* 7.4, 2504 transients (1.39 h per time point). Leucine-14 is not visible at this pH. The data for leucine-41 fit well to an exponential decay [inset (●)] with k_{ex} = (2.40 ± 0.06) × 10^{-5} s^{-1}. In both plots, the intensity of the leucine-41 resonance at time = 0 was normalized to a value of 100.

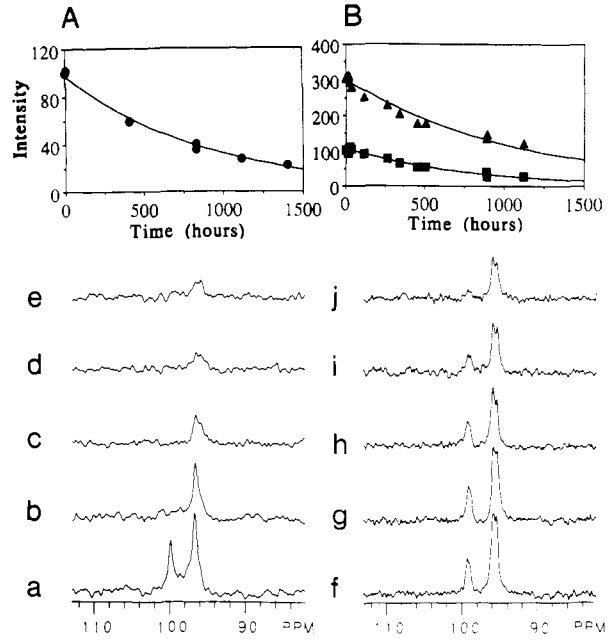

FIGURE 4: Representative ^{15}N INEPT NMR spectra from time-dependent exchange-out experiments in ^2H_2O buffer measured over an extended period of time. (A) [^{15}N]Leucine-labeled coat protein in SDS micelles, pH* 2.52, 10-Hz line broadening; 5000 transients were averaged for each point: (a) 1.46, (b) 407, (c) 829, (d) 1112, and (e) 1400 h. Leucine-14 exchanges comparatively fast at this pH* and is only visible in spectrum a. The intensity of leucine-41 decays as a first-order process (inset) with a rate constant (k_{ex}) of (3.25 ± 0.13) × 10^{-7} s^{-1}. The plotted intensities were normalized to a value of 100 at zero time, and the data were corrected as described under Methods. (B) [^{15}N]Valine-labeled coat protein in SDS, pH* 6.62, 5-Hz line broadening: (f) 1.46, (g) 110, (h) 250, (i) 506, and (j) 800 h. The intensities of both valine-A (■) and valine-B (▲) fitted to single-exponential decays (inset) with k_{ex} values of (3.69 ± 0.13) × 10^{-7} and (2.59 ± 0.16) × 10^{-7} s^{-1}, respectively. The fitted data were normalized to a value of 300 for valine-B.

signed by labeling the peptide bond between glycine-23 and tyrosine-24 with ^{13}C (glycine carbonyl) as well as ^{15}N (tyrosine amide) and observing the spin coupling (see Figure 2, inset); the downfield resonance arises from tyrosine-24. Glycine-3 (Figure 2) was assigned on the basis of its very narrow line width in comparison with the previously assigned distinctive narrow carbonyl resonance of this residue (Henry et al., 1987a). This resonance also has a strong negative NOE in directly detected ^{15}N spectra (Henry & Sykes, 1987c; Bogusky et al., 1988). The other three glycine resonances give rise to multiple peaks [see Henry and Sykes (1990a,b)]; these were not assigned and were not included in this study.

Amide Exchange in ^2H_2O. Amide exchange rates were determined as a function of pH* in ^2H_2O for the leucine, valine, and tyrosine residues. Both leucine amides exchange slowly enough to be detected by direct exchange-out at 23 °C, but leucine-14 is near the upper limit of detection so that only rates close to the pH* minimum can be measured. Figure 3a shows a typical exchange-out profile of leucine-14 at pH* 3.5 which was obtained over a time period of about 15 h after protonated protein was dissolved in buffered ^2H_2O; note the constant intensity of leucine-41 which exchanges very slowly at this pH* value. The exchange of leucine-41 over a similar time scale required a pH* of 7.4 (Figure 3b). Leucine-14 exchanges almost instantaneously at this pH* and is not visible in the INEPT spectrum. Amide exchange rates of leucine-41 at lower pH* values were obtained by measuring the ^{15}N INEPT intensity on different occasions over a period of weeks or months as necessary. Figure 4a–e shows spectra of leucine-41 at pH* 2.5 obtained over a longer time period. The valine amides in the center of the hydrophobic region are among the slowest residues in the coat protein to exchange; many months were required to measure rates at pH values around the rate minimum. All of the valine amides appear to exchange at approximately similar rates, and their time-dependent exchange at pH* 6.6 is illustrated in Figure 4f–j. Data for the peak designated valine-B, which is composed of three individual resonances, fitted well to a single exponential at all pH values. Both tyrosine residues, like leucine-14, exchange rapidly on the time scale of an exchange-out experiment, and k_{ex} can be measured only near the pH* minimum. A typical experiment at pH* 5.0 is shown in Figure 5 where tyrosine-21 can be seen to exchange slightly faster than tyrosine-24. Glycine-3 exchanges much too rapidly to be measured in a direct exchange-out experiment. For all these labels, exchange rates were determined at a given pH by fitting the data to a single-exponential decay; examples are shown in Figures 3–5.

The exchange rates of leucine-14, leucine-41, tyrosine-21, tyrosine-24, valine-A, and valine-B as a function of pH were fitted to eq 1 using a nonlinear least-squares fitting routine (Figure 6). The k_D, k_{OD}, and pH_{min} values and retardations with respect to poly(DL-alanine) thus obtained are collected in Table I. All these amides, as expected, exchange much more slowly than poly(DL-alanine) (at least in the base-catalyzed regime), and excellent fits to eq 1 were obtained. However, a substantial shift in the pH* minimum value (up to 1.5 pH units) is also observed. The shift is smallest for leucine-14 and largest for the valine residues of the hydrophobic core (see Discussion). The shape of the curve for the more slowly exchanging residues does not deviate significantly

Table I: Exchange Parameters Calculated from Experimental Data

residue	k_D (M^{-1} s^{-1})[a]	k_{OD} (M^{-1} s^{-1})[a]	k_{OH} (M^{-1} s^{-1})[a]	method	corrected $k_{OH/OD}$ (M^{-1} s^{-1})[b]	pH^*_{min}[c]	retardation $1/K_{op}$[d]
glycine-3			(9.4 ± 1.0) 10^7	polarization transfer	3.3×10^7 (k_{OH})		1.0
			$(7.4 \pm 0.6) \times 10^7$	saturation transfer	2.6×10^7 (k_{OH})		1.3
leucine-14	$(4.9 \pm 1.1) \times 10^{-2}$	$(2.4 \pm 0.5) \times 10^6$		exchange-out	1.2×10^5 (k_{OH})	4.0 (3.6)	245
			$(3.0 \pm 0.7) \times 10^5$	saturation transfer	1.5×10^6 (k_{OD})		230
tyrosine-21	$(6.0 \pm 1.5) \times 10^{-1}$	$(1.5 \pm 0.5) \times 10^6$		exchange-out	9.5×10^5 (k_{OD})	4.4 (4.3)	310
tyrosine-24	$(3.7 \pm 1.2) \times 10^{-1}$	$(5.5 \pm 2.4) \times 10^5$		exchange-out	6.9×10^5 (k_{OD})	4.5 (4.4)	425
valine-A	$(9.2 \pm 2.1) \times 10^{-5}$	$(6.5 \pm 1.2) \times 10^1$		exchange-out	6.5×10^1 (k_{OD})	4.5	4.6×10^6
valine-B	$(3.3 \pm 0.9) \times 10^{-5}$	$(4.3 \pm 0.9) \times 10^1$		exchange-out	4.3×10^1 (k_{OD})	4.4	6.9×10^6
leucine-41	$(1.3 \pm 0.2) \times 10^{-4}$	$(5.4 \pm 1.0) \times 10^2$		exchange-out	2.7×10^2 (k_{OD})	4.5 (4.1)	1.1×10^4

[a] k_D and k_{OD} are acid- and base-catalyzed rate constants in ^2H_2O; k_{OH} values were measured in water. Values were obtained directly from fits to experimental data; $pK_w = 14.06$, $pK_{D_2O} = 14.92$. The errors are the standard deviations of the fits. [b] Corrected for sequence effects using the model peptide data of Molday et al. (1972). [c] Calculated from eq 2 using Molday corrected k_{OD} and k_D values; uncorrected values are in parentheses. [d] $k_{OD} = 2.87 \times 10^8$; $k_{OH} = 3.43 \times 10^7$.

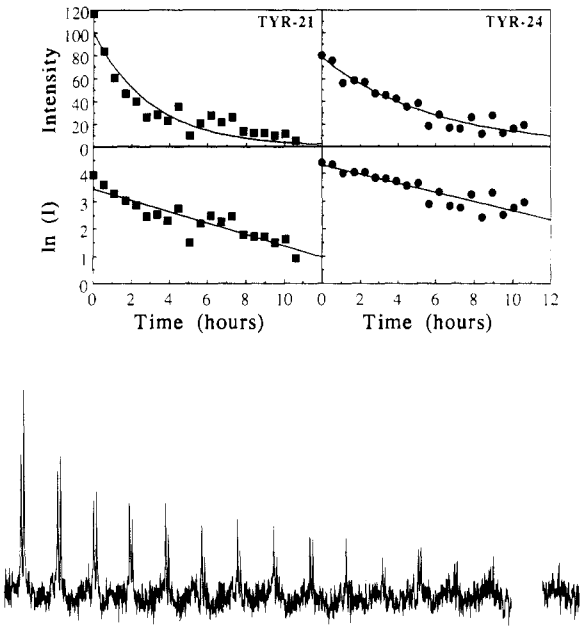

FIGURE 5: Time-dependent decay of the ^{15}N INEPT NMR signal of [^{15}N]tyrosine-labeled coat protein in ^2H_2O, pH* 5.0; 1000 transients were averaged (0.55 h per time point), and a line broadening of 5 Hz was applied. The isolated data point is the spectrum acquired after 10.64 h (corresponding to the final point on the graphs) and shows that tyrosine-21 (upfield peak) has disappeared and tyrosine-24 is very small. The signal intensities were normalized to a value of 100 for tyrosine-21, and the decays were fitted to single exponentials (upper panels of inset), yielding rate constants of $(9.10 \pm 0.11) \times 10^{-5}$ (■) and $(4.86 \pm 0.36) \times 10^{-5}$ s^{-1} (●) for tyrosines-21 and -24, respectively. Logarithmic plots, presented in the lower panels, result in straight lines showing that a single-exponential fit is reasonable. However, the tyrosine-21 data possess a large amount of scatter as the exchange rates are close to the fast limit for this type of experiment; more than half at the points are obtained from signal intensities which are comparable with the spectral noise. Furthermore, it can be seen that the base line is not completely flat around the tyrosine signals (probably due to low levels of nonspecific labeling), contributing further to the inaccuracy of time points obtained near the end of the experiment. Errors in these points are enhanced by a linear fit, resulting in a slope which does not give the best estimate of the rate constant. For these reasons, nonlinear least-squares fitting to the exponential decay is to be preferred.

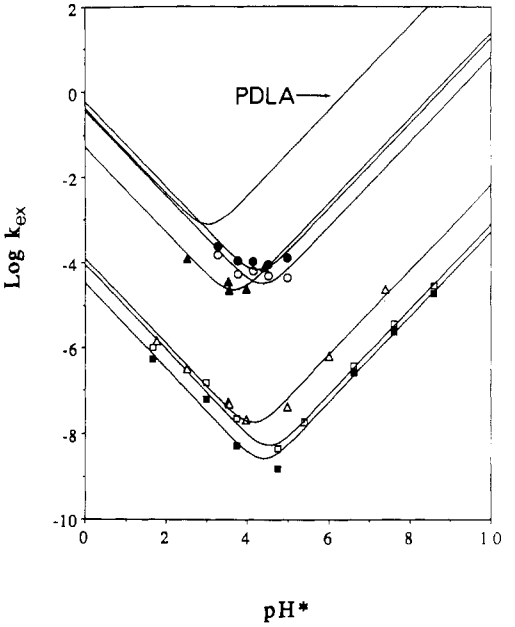

FIGURE 6: Log rate as a function of pH* for valine-A (□), valine-B (■), leucine-41 (△), leucine-14 (▲), tyrosine-21 (●), and tyrosine-24 (○). The data were fitted by using eq 1 with pK_{D_2O} taken to be 14.92 (Covington et al., 1966). The line labeled PDLA was calculated for the unstructured polypeptide poly(DL-alanine) using $k_{OD} = 2.97 \times 10^8$ and $k_D = 0.421$ M^{-1} s^{-1} (see Methods).

from that of poly(DL-alanine), unlike some rate vs pH curves observed for residues in other proteins such as the basic pancreatic trypsin inhibitor (Richarz et al., 1979; Hilton & Woodward, 1979). This is probably due to the lack of ionizable groups in the coat protein over the pH range of study; all of the carboxyl groups except that of glutamic acid-20 occur in the mobile terminal regions. No evidence for pH-independent catalysis by water (Gregory et al., 1983) was apparent either for the valine residues or for leucine-41.

Amide Exchange in ^1H_2O. As described under Theory, the ^{15}N INEPT experiment can also be used to monitor moderately fast amide exchange rates ($k_{ex} \cong 1/T_{1,amide}$) in a saturation transfer experiment performed in water. This is not conventional saturation transfer as both the amide proton and water are saturated during proton decoupling (eq 3; Forsen & Hoffman, 1963). Nevertheless, as k_{ex} approaches the amide proton relaxation rate, the intensity of the INEPT signal diminishes unless the delay between transients is substantially greater than $T_{1,water}$ (≅3.3 s). Such an experiment is illustrated in Figure 7a for glycine-3 as a function of pH using a moderate recycle delay (1 s); the intensity of glycine-3 decreases as k_{ex} increases, whereas the intensity of the more slowly exchanging upfield glycines remains constant. If sufficient time is left for the water signal to recover, however, then no transfer of saturation can occur. For example, the full intensity of glycine-3 is seen at pH 7 if a 30-s relaxation delay is used (Figure 7b), whereas only 50% of the original intensity remains as this pH in Figure 7a. Nevertheless, even in the presence of a long delay, the INEPT signal is eventually lost as k_{ex} increases; in this limit, it is due solely to exchange-induced loss of phase information during the four $1/(4J)$ delays in the pulse sequence. This situation is simpler to analyze and will be con-

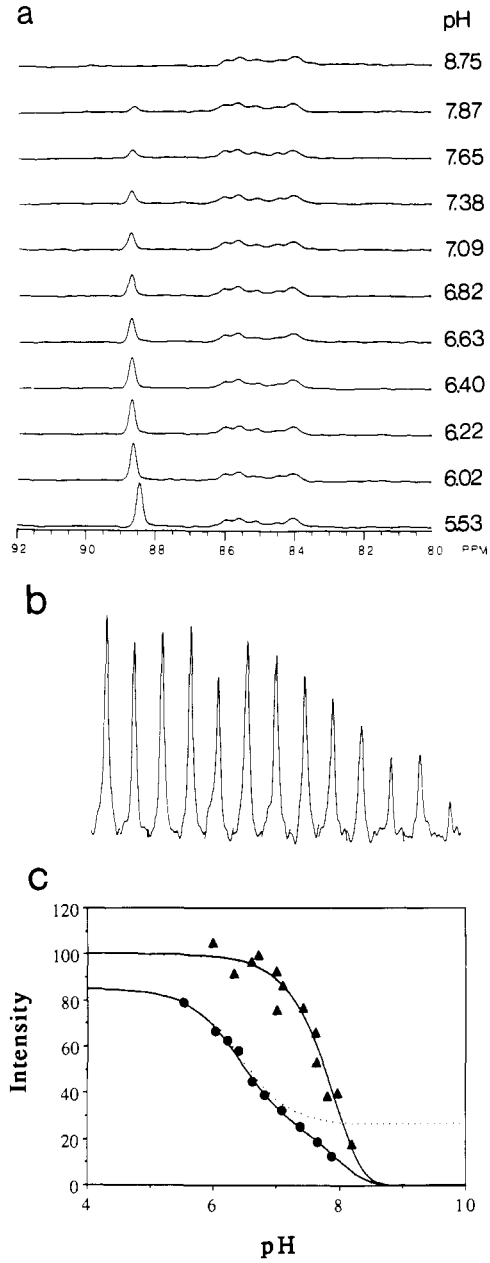

FIGURE 7: pH titration of [^{15}N]glycine-labeled coat protein in SDS micelles. (a) ^{15}N INEPT NMR spectra recorded with a relaxation delay of 1.0 s; 5000 transients were averaged, and the free induction decay was multiplied by a Lorentzian to Gaussian function to enhance resolution. Glycine-3 undergoes a slight upfield shift at low pH values, probably due to ionization of the adjacent aspartic acid residues. (b) ^{15}N INEPT NMR spectra (only glycine-3 is shown) recorded with a relaxation delay of 30 s. A total of 256 transients were averaged, and a line broadening of 10 Hz was used. pH values from left to right are 6.00, 6.33, 6.61, 6.72, 7.01, 7.11, 7.42, 7.62, 7.64, 7.82, 7.98, and 8.20. (c) Plot of INEPT intensity vs pH for glycine-3. Peak heights from (b) [30-s delay (▲)] are fitted by using eq 4; a k_{OH} value of $(9.37 \pm 0.97) \times 10^7$ M^{-1} s^{-1} was obtained. Peak heights from (a) [1-s delay (●)] are fitted by using a combination of eq 3 and 4, yielding a k_{OH} value of $(7.37 \pm 0.57) \times 10^7$ M^{-1} s^{-1}. The dotted line is the intensity to be expected in the presence of saturation transfer only. Constants were as follows: $T_{1,amide} = 0.53$ s, $T_{1,water} = 3.3$ s, $J_{NH} = 94.5$ Hz, $pK_w = 14.06$.

sidered first. Signal intensity in the absence of saturation transfer depends only on the exchange rate, k_{ex}, and the coupling constant, J_{NH}, according to eq 4. For typical J_{NH} values of 95 Hz, when $k_{ex} = J_{NH} = 95$ s^{-1}, $I = 0.368I_0$. The base-catalyzed rate constant for glycine-3 (k_{OH}) was determined to be 9×10^7 M^{-1} s^{-1} by fitting the pH-dependent intensities of Figure 7b to eq 4 (Figure 7c).

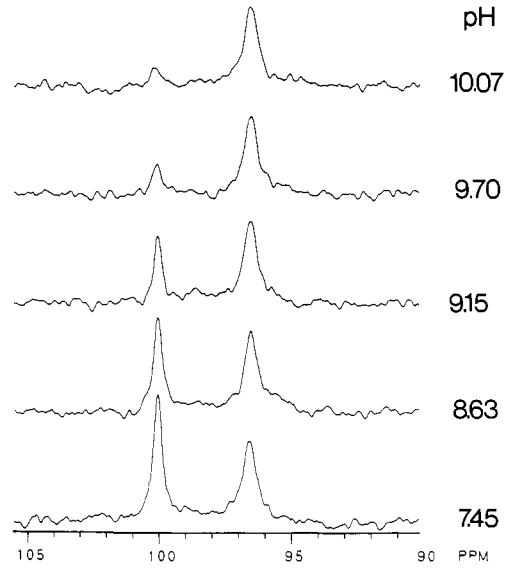

FIGURE 8: Intensity of ^{15}N INEPT NMR signals for [^{15}N]leucine-labeled coat protein in SDS micelles in ^1H_2O buffer as a function of pH. Leucine-14 decreases in intensity with increasing pH, but leucine-41 remains constant.

Although easy to quantify, the long delays between transients (which are necessary to allow the water to recover) make the above experiment very time-consuming, and the signal to noise ratio, even in this favorable case, is poor. Predicting the intensities obtained at short relaxation delays offers a more practical method for determining rate constants. It can be seen from Figure 7 that the exchange regimes affected by saturation transfer and polarization transfer are not completely distinct (significantly longer $T_{1,amide}$ values would be required for this to be the case). The glycine-3 intensity does not level off at constant value as $T_{1,water}$ becomes dominant; instead, the intensity falls to zero as exchange effects on the polarization transfer step become important. The intensity of a given resonance at short recycle delays thus depends on a combination of eq 3 and 4 and requires a knowledge of both $T_{1,amide}$ and $T_{1,water}$. The T_1 of the glycine-3 amide proton was determined to be 0.53 s by varying the recycle delay at low pH values (4.5–5.0), i.e., an experiment equivalent to T_1 measurement by progressive saturation. A fit to the experimental data of Figure 7a (1-s delay) is shown together with the 30-s delay data in Figure 7c. An excellent fit was obtained in which the biphasic nature of the events is readily apparent. k_{OH} was found to be 7×10^7 M^{-1} s^{-1}, in good agreement with the value obtained from the long delay experiment. Both sets of data in Figure 7c were normalized to a maximum z magnetization value (I_0) of 100. This is realized when the relaxation delay is long, but the intensity obtained at short delays is partially saturated; the maximal observable intensity with a 1-s delay falls to 85% of the original. The dotted line in Figure 7c corresponds to intensity in the presence of saturation transfer alone (eq 3), calculated by using the fitted value for k_{OH}. The theory of this type of experiment will be discussed more fully elsewhere (Henry and Sykes, unpublished results).

A similar saturation transfer experiment was performed on the amide proton of leucine-14 (Figure 8); the intensity of leucine-14 decreases as k_{ex} increases, whereas the intensity of the slowly exchanging leucine-41 remains constant. The amide proton T_1 of leucine-14 was found to be 0.50 s^{-1} at low pH, and the intensity was fitted with a k_{OH} value of 3×10^5 s^{-1} (data not shown). This is apparently about 10-fold slower than the k_{OD} value obtained by direct exchange-out in ^2H_2O; however, the difference is similar to the difference in rate

constants obtained with model peptides under similar conditions. The retardation values ($1/K_{op}$) concur when these isotope effects are taken into account (Table I).

Discussion

Application of ^{15}N NMR to Quantitation of Amide Hydrogen Exchange Rates. The ^{15}N isotope is becoming increasingly popular in NMR studies of macromolecules; recent applications (neglecting solid-state work) include exploitation of the negative gyromagnetic ratio to locate regions of independent local motion through negative NOe values, determination of proton chemical shifts through heteronuclear shift correlation, and the editing of proton spectra (e.g., Bogusky et al., 1985, 1988; Griffey et al., 1985; Shiksnis et al., 1987; Smith et al., 1987; McIntosh et al., 1987; Leighton & Lu, 1987; Stockman et al., 1988; and Torchia et al., 1988). Here, we have explored the use of ^{15}N NMR to quantitate amide hydrogen exchange kinetics in M13 coat protein. Previous experiments from this laboratory, which used ^1H NMR to follow exchange of the broad amide proton envelope of SDS-solubilized coat protein, located a number of slowly exchanging amides within the hydrophobic region of the molecule (O'Neil & Sykes, 1988). The long correlation time of the protein–detergent complex results in unfavorably broad lines; thus, individual amides cannot be observed readily by ^1H NMR. Isotope labeling can provide resolution (e.g., Kainosho & Tsuji, 1985; Griffey et al., 1985), and a ^{13}C isotope shift technique (Henry et al., 1987b) allowed us to measure individual rates for many amides in the hydrophilic domains of the protein. However, this method is useful only for relatively fast rates (k_{ex} = 2–125 s^{-1}). The ^{15}N INEPT experiment provides access to a number of exchange regimes and could be used to obtain a rate profile for the entire protein if necessary. Of course, the principles discussed here are not unique to the INEPT experiment, but should be equally applicable to decoupled DEPT (Doddrell et al., 1982) or directly detected $^{15}N/^1H$ heteronuclear shift correlation. Experiments which are conceptually similar to these have been performed using ^{15}N-edited ^1H spectroscopy by Griffey et al. (1985) for five phenylalanine resonances in T_4 lysozyme and by McIntosh et al. (1987) using uniform ^{15}N labeling in the same protein. The refocused INEPT sequence performs better than the alternative DEPT experiment because it is $1/(2J)$ s (5.3 ms) shorter; this is important for proteins where T_2 values can be inconveniently short.

Analysis of Amide Exchange Rates. Little is known about the structural fluctuations which give rise to the exchange event, but two extreme models are currently contested. The solvent penetration model requires diffusion of the catalytic ions to the protein interior through transiently forming channels; exchange rates are predicted to depend on the depth or extent of burial. The local unfolding model assumes that slowing is due to the formation of stable hydrogen bonds and that exchange takes place from a transiently open or unfolded state. Open states are proposed to be small (10 residues or less) except under conditions approaching whole molecule denaturation (Woodward et al., 1982; Barksdale & Rosenberg, 1982; Englander & Kallenbach, 1984). These models have proved remarkably difficult to distinguish, and data on individual protons in proteins are very limited. Nevertheless, it appears that internal hydrogen bonding is responsible to a significant degree for retardation of exchange in the N-terminal helices of cytochrome *c* (Wand et al., 1985) and ribonuclease S (Kuwajima & Baldwin, 1983). The importance of hydrogen bonding has also been emphasized in neutron diffraction studies (e.g., Kossiakoff, 1982). In concordance with our previous work (Henry et al., 1987b; O'Neil & Sykes, 1988), we have chosen to interpret our results in terms of the local unfolding model. The following scheme applies to the direct exchange-out experiment (Hvidt & Neilsen, 1966):

$$N(H) \underset{k_2}{\overset{k_1}{\rightleftharpoons}} O(H) \xrightarrow[k_3]{k_3} O(^2H) \underset{k_1}{\overset{k_2}{\rightleftharpoons}} N(^2H)$$

where N and O refer to the native and open forms, respectively. k_3 is equivalent to the rate of exchange in an unstructured peptide. Assuming $k_2 \gg k_1$ (i.e., the native form is more stable than the open form), the following equation can be derived for the exchange rate at constant pH:

$$k_{ex} = k_1k_3/(k_2 + k_3) \quad (5)$$

Two limits may be observed; if $k_3 \gg k_2$ (EX1 kinetics), then $k_{ex} = k_1$, and exchange is independent of pH. When $k_2 \gg k_3$ (EX2 kinetics), as is usually the case, $k_{ex} = K_{op}k_3$. Only the equilibrium constant of the opening reaction ($K_{op} = k_1/k_2$) may be determined as the intrinsic exchange rate, k_3, is now rate-limiting. Under these circumstances, k_{ex} is pH dependent. All of the amide protons observed in M13 coat protein exhibit EX2 kinetics. The retardation of the exchange rate, relative to the standard model compound poly(DL-alanine), is equivalent to k_{ex}/k_3 or $1/K_{op}$, the inverse of the opening equilibrium constant (Roder et al., 1985a). k_3 corresponds to the rate of a freely exposed peptide and may be calculated from the k_H and k_{OH} values measured for poly(DL-alanine) (Englander et al., 1979) as described under Methods. Small nearest-neighbor inductive effects occur in proteins, largely due to electron-withdrawing side chains. These make the amide a stronger acid, thus enhancing base catalysis and diminishing acid catalysis. Correction factors for k_3 were determined in a model compound study by Molday et al. (1972), and the validity of the application has been well verified (Roder et al., 1985b).

Retardation of Amide Exchange Rates and the Structure of M13 Coat Protein in SDS Micelles. The retardation of exchange rates with respect to poly(DL-alanine) ($1/K_{op}$) is summarized in Table I. No correction was made for the shifts in the pH minima from the standard poly(DL-alanine) value of 3.0, although clearly this may affect the true retardation. Possible reasons for the pH_{min} shift will be discussed later. Individual values are of variable accuracy; for example, numbers obtained for the valine residues and leucine-41 should be close to the actual values, as both acid- and base-catalyzed limbs of the rate vs pH curve are well-defined. Values measured for leucine-14 (in D_2O), tyrosine-21, and tyrosine-24, by contrast, will be less reliable. Similarly, the retardation observed previously for leucine-41 in a ^{13}C isotope shift experiment (Henry et al., 1987b) is less likely to be a good reflection of the actual value since it was determined from a single point at a high pH value (pH ≈12). This is at the extreme limit of the isotope shift experiment, and the ^{15}N data did, in fact, return a value approximately 3-fold slower.

The secondary and tertiary structures of detergent-solubilized M13 coat protein are not known. Circular dichroism spectra of the coat protein solubilized in SDS, deoxycholate, or lysophosphatidylcholine micelles are quite similar and indicate about 50% α-helical structure and 30% β-sheet (Nozaki et al., 1976). These studies are compatible with more recent NMR work which suggests approximately eight residues to be unstructured, perhaps four from each end of the molecule. The evidence for this is quite extensive and includes α-carbon and carbonyl carbon line widths (Cross & Opella, 1980; Henry et al., 1987a), quantitative ^{13}C relaxation measurements on alanine methyl carbons (Henry et al., 1986), large negative nuclear Overhauser enhancements in directly detected ^{15}N

spectra (Bogusky et al., 1985, 1988), and amide hydrogen exchange rates similar to those of model peptides (Henry et al., 1987b). By contrast, the rest of the protein appears to be largely immobile on the time scale of NMR relaxation ($\tau_c \cong$ 10 ns). Amide hydrogen exchange is sensitive to events which may occur on a much slower time scale than relaxation, but equilibrium constants rather than rate constants are obtained under conditions of EX2 kinetics. The results of these experiments are fully compatible with those obtained earlier (Henry et al., 1987b; O'Neil & Sykes, 1988) and help to give a clearer picture of the protein. Glycine-3 was found to exchange at the poly(DL-alanine) rate, as do other mobile residues (glutamic acid-2 and serine-50). Reasonably fast rates ($1/K_{op}$ = 10–500) are found in much of the "immobile" part of the N-terminal region (e.g., leucine-14), whereas most amides of the hydrophobic core are slow (Henry et al., 1987b; O'Neil & Sykes, 1988). However, the location of the slowest amides in the coat protein appears to be offset to some extent from the center of the hydrophobic sequence, extending into the C-terminal hydrophilic region; the tyrosine residues (tyrosines-21 and -24) at the start of the hydrophobic sequence, for example, exchange surprisingly fast and at a rate comparable with threonine-46. In line with current thinking on membrane protein structure [see Engelman (1985)] and taking retardation of exchange as an indication of the presence of hydrogen bonding, these results are consistent with a model in which the hydrophobic core is helical and extends almost to the C-terminus, where it undergoes dynamic fraying. The structure of the N-terminal region is uncertain but is proposed to be in a state of relatively rapid dynamic flux. These motions are too infrequent to influence ^{13}C relaxation.

Location of Bound SDS. Protein–detergent interactions have been studied extensively by Tanford and co-workers. Water-soluble proteins (and some membrane proteins) normally bind SDS in a fixed weight to weight ratio to form a rod of uniform charge density (Reynolds & Tanford, 1970); SDS alters the conformation of these proteins and binds cooperatively to the denatured state. The association involves SDS monomers (not micelles), and the amount of bound detergent is independent of ionic strength. Different results are obtained with small hydrophobic proteins. The coat protein from the filamentous phage fl (which differs by one residue from that of M13) interacts with SDS in an ionic strength dependent and highly cooperative fashion near the critical micelle concentration (Makino et al., 1975; Nozaki et al., 1978). These authors suggested that rather than associating with SDS monomers like most water-soluble proteins, the hydrophobic region of the coat protein acts as a nucleus for micelle binding. The size and shape of the protein-bound micelle are proposed to resemble the micelle in the absence of protein. Cooperative denaturation by SDS thus need not occur for the small hydrophobic membrane protein which can bind more SDS by associating with a micelle in the "native" (i.e., the so-called 50% α-helical) state than it can in the denatured state (Nozaki et al., 1978). Comparable results have been obtained for cytochrome b_5, another small integral membrane protein, and its proteolytic subfragments (Robinson & Tanford, 1975). A picture of the coat protein in which an SDS micelle mimics the lipid bilayer is therefore not unreasonable. In further support of such a model, we have previously shown that the hydrophobic region of SDS (or deoxycholate) solubilized coat protein is highly protected from digestion by proteinase K (a protease of low specificity) whereas the N-terminal domain was very rapidly removed (Henry et al., 1987a; G. D. Henry and B. D. Sykes, unpublished data).

Effects of Bound Detergent on Amide Exchange Rates. No amides in the coat protein exchange more than 10^6-fold more slowly than poly(DL-alanine) (O'Neil & Sykes, 1988); therefore, the four valine residues (29, 30, 31, 33) must be among the slowest in the protein. This raises the question as to how the detergent-bound hydrophobic region becomes exposed to water and catalytic ions in order for exchange to take place. Even the slowest amides in M13 coat protein (10^6-fold retardation) are much faster than the β-sheet protons of the basic pancreatic trypsin inhibitor (Wagner, 1983) and the N-terminal helix of cytochrome *c* (Wand et al., 1985); thus, it would seem that the detergent does not present a major barrier to exchange.

Various aspects of micelle structure, such as water content, surface charge, counterion association, size, stability, and alkyl chain dynamics, are all potentially relevant to amide hydrogen exchange kinetics in micelle-bound coat protein; yet, the structure of micelles is still a subject of considerable controversy [Menger & Doll, 1984; Dill et al., 1984; see also Fendler (1982)]. ^{13}C NMR relaxation times show that a gradient of segmental motion, greatest at the terminal methyl, exists along the alkyl chain in SDS (Roberts & Chachaty, 1973). Furthermore, micelles are inherently dynamic structures, undergoing continual break up and re-formation; the lifetime of a typical micelle is probably much shorter than the measured exchange lifetimes. In this light, it seems reasonable to suggest that local unfolding of the polypeptide chain in the hydrophobic region, which is required to expose the amide protons for exchange, might be accompanied by substantial transient disruption of the whole micelle. Even if the local unfolding reaction was of more modest extent, there appears to be a reasonable amount of water available *within* a micelle (Casal, 1988). A hydrophobic tripeptide, Leu-Val-Ile-NH_2, was designed to monitor hydrogen exchange rates in the micelle interior (O'Neill & Sykes, 1989a). The peptide did not experience any retardation in exchange rate when associated with an SDS micelle, although the effect of surface charges produced a substantial shift in the pH of minimum rate (see later).

Origin of pH_{min} Shifts. Multiexponential analysis of the amide proton envelope observed by ^1H NMR suggested that a significant number of amides in the protein undergo a basic shift in the pH of their rate minima (pH_{min}) when compared with poly(DL-alanine) (O'Neil & Sykes, 1988). We have now confirmed the existence of considerable pH_{min} shifts for individual amides in the hydrophobic region (1.5 pH units for valine residues and 1.2 pH units for leucine-41). The smallest shift was observed for leucine-14 in the N-terminal hydrophilic region (0.5 pH unit).

Suppression of K_w, which occurs upon addition of less polar solvents, causes both an apparent basic shift and a depression of pH_{min} in model amides. This is an artifact caused by direct measurement of pH rather than pOH (Leichtling & Klotz, 1966). Such an argument does not apply to proteins (or to the micelle-bound coat protein), however, as thermodynamic equilibrium is established through the entire solution and K_w must remain constant throughout (Perrin & Lollo, 1984). Kim and Baldwin (1982) showed that long-range electrostatic effects are important in the hydrogen exchange chemistry of positively charged poly(DL-lysine), causing an acid shift in the pH_{min} of 1.4 pH units in the presence of 50 mM sodium chloride. This was attributed to condensation of anions (including small but significant amounts of OH^-) at the polymer surface. Similar counterion condensation at the surface of micelles is well-documented [see Fendler (1982)], and a basic shift would be expected for amides associated with SDS, which

has a negative charge. In a model compound study designed to assess the effects of bound detergent, the amides of the hydrophobic tripeptide Leu-Val-Ile-NH_2 were observed to undergo substantial basic pH_{min} shifts (1.3–1.8 pH units) when solubilized by SDS micelles (O'Neill & Sykes, 1989a). No depression of the pH_{min} was observed, however, and it was concluded that in this system the shift could be accounted for solely in terms of long-range electrostatic attraction of protons to the micelle. The small shift in the pH_{min} of leucine-14 amide might be accounted for by such electrostatic effects as the cation-rich layer (Gouy-Chapman layer) extends for some considerable distance beyond the micelle surface. The side chain amide of the adjacent residue, glutamine-15, undergoes a 1.5 pH unit basic shift but no retardation, suggestive of electrostatic effects alone (O'Neil & Sykes, 1989b). Of course, nearby glutamic and aspartic acid side chains might also contribute.

Although the positively charged peptide in the model compound study was clearly micelle-bound, its location within the micelle is not known. It has been suggested that polar probe molecules are generally associated with the water-rich region near the polar head groups (Stern region). The situation for the micelle-bound region of the coat protein may well be more complex and not explicable in terms of electrostatic effect alone. Perrin and Lollo (1984) suggested a mechanism for basic pH_{min} shifts in proteins which should apply equally well to the micelle-solutilized coat protein. Base-catalyzed exchange occurs via abstraction of the amide proton, proceeding through a negatively charged transition state. The mechanism of acid catalysis is more controversial; Perrin and Lollo concluded that acid catalysis in peptides occurs via protonation of the carbonyl oxygen (O-protonation or imidic acid mechanism) and that this transition state is uncharged. The presence of the hydrophobic SDS molecules would thus enhance acid catalysis by stabilization of the uncharged transition state, and depress base catalysis through their inability to solvate the negative charge. The net results is both a shift and a depression of the pH minimum. Micelles are well-known to catalyze simple chemical reactions, such as the hydrolysis of esters or amides, through similar charge or hydrophobic effects [see Jencks (1969)]. It seems likely that the pH_{min} shifts in M13 coat protein result from a combination of both charge effects, which cause a shift only, and the above-mentioned hydrophobic effects, which cause both a shift and a depression. Both mechanisms make retardations of amide exchange rates (calculated from k_{OH} values) appear to be greater than they really are; however, it is impossible to apply corrections to $1/K_{op}$ without knowing the relative extent of the contributions. It should be possible to resolve these effects to some extent by using an uncharged detergent such as octyl glucoside. Unfortunately, the coat protein is considerably less stable in octyl glucoside micelles and gradually precipitates over the long time periods required to obtain measurable amide exchange rates.

One final point concerns the M13 coat protein dimer. In a recent publication (Henry & Sykes, 1990b), we have suggested the dimer to be asymmetric (i.e., the monomers are not identical), as a number of ^{13}C-labeled carbonyl carbons and ^{15}N-labeled backbone amides give rise to two resonances of equal intensity (the latter experiment, performed at 50.6 MHz for ^{15}N, revealed splittings which are not apparent at 30.4 MHz). Furthermore, using a ^{13}C NMR isotope shift method (Henry et al., 1987b) to measure rapid amide hydrogen exchange under circumstances where the individual monomers are clearly resolved, it was shown that slightly different exchange rates (approximately 2-fold) exist at the two sites (G. D. Henry and B. D. Sykes, unpublished results). Other experiments, however, show the monomers themselves to exchange on a time scale of the order of seconds or less (G. D. Henry and B. D. Sykes, unpublished data). Thus, although a difference in exchange rates may be observed for the two monomers if hydrogen exchange exceeds the rate of monomer interchange, most of these experiments would be expected to reflect only time-averaged rates.

Acknowledgments

We thank Gerry McQuaid for constructing the ^{15}N probe used in these experiments and for continued maintenance of the NMR spectrometer, Dr. Joe O'Neil for numerous discussions, Dr. Joel Weiner for providing facilities for growing *E. coli* cells and phage purification, and the Medical Research Council of Canada for financial support. Helpful discussions with Dr. S. J. Opella are also acknowledged with pleasure.

Registry No. SDS, 151-21-3; hydrogen, 1333-74-0; deuterium, 7782-39-0.

References

Asbeck, F., Beyreuther, K., Kohler, H., von Wettstein, G., & Braunitzer, G. (1969) *Hoppe-Seyler's Z. Physiol. Chem. 350*, 1047–1056.

Barksdale, A. D., & Rosenberg, A. (1982) *Methods Biochem. Anal. 28*, 1–113.

Blomberg, F., & Rüterjans, H. (1978) in *Nuclear Magnetic Resonance Spectroscopy in Molecular Biology* (Pullman, B., Ed.) p 231, Reidel, Dordrecht, The Netherlands.

Boelens, R., Gros, P., Sheek, R. M., Verpoorte, J. A., & Kaptein, R. (1985) *J. Biomol. Struct. Dyn. 3*, 269–280.

Bogusky, M. J., Leo, G. C., & Opella, S. J. (1985) in *Magnetic Resonance in Biology and Medicine*, XI International Conference on Magnetic Resonance in Biological Systems, Tata McGraw-Hill Publishing Co. Limited, New Delhi.

Bogusky, M. J., Leo, G. C., & Opella, S. J. (1988) *Proteins: Struct., Funct., Genet. 4*, 123–130.

Casal, H. L. (1988) *J. Am. Chem. Soc. 110*, 5203–5205.

Cavalieri, S. J., Goldthwaite, D. A., & Neet, K. E. (1976) *J. Mol. Biol. 102*, 713–722.

Covington, A. K., Robinson, R. A., & Bates, R. G. (1966) *J. Phys. Chem. 70*, 3820–3824.

Cross, T. A., & Opella, S. J. (1980) *Biochem. Biophys. Res. Commun. 92*, 478–484.

Cross, T. A., & Opella, S. J. (1981) *Biochemistry 20*, 290–297.

Cross, T. A., & Opella, S. J. (1985) *J. Mol. Biol. 182*, 367–381.

Datema, K. P., Visser, A. J. W. G., van Hoek, A., Wolfs, C. J. A. M., Spruijt, R. B., & Hemminga, M. A. (1987) *Biochemistry 26*, 6145–6152.

Dempsey, C. E. (1986) *Biochemistry 25*, 3904–3911.

Dettman, H. D., Weiner, J. H., & Sykes, B. D. (1984) *Biochemistry 23*, 705–712.

Dill, K. A., Koppel, D. E., Cantor, R. S., Dill, J. D., Bendedouch, D., & Chen, S.-H. (1984) *Nature 309*, 42–45.

Doddrell, D. M., Pegg, D. T., & Bendall, M. R. (1982) *J. Magn. Reson. 48*, 323–327.

Engelman, D. M., Steitz, T. A., & Goldman, A. (1986) *Annu. Rev. Biophys. Biophys. Chem. 15*, 321–353.

Englander, J. J., Calhoun, D. B., & Englander, S. W. (1979) *Anal. Biochem. 92*, 517–524.

Englander, S. W., & Poulsen, A. (1969) *Biopolymers 7*, 329–339.

Englander, S. W., & Kallenbach, N. R. (1984) *Q. Rev. Biophys. 16*, 521–655.

Fendler, J. H. (1982) in *Membrane Mimetic Chemistry*, Wiley, New York.
Forsen, S., & Hoffman, R. A. (1963) *J. Chem. Phys. 40*, 1189–1196.
Glasoe, P., & Long, F. (1960) *J. Phys. Chem. 64*, 188–190.
Gregory, R. B., Crabo, L., Percy, A. J., & Rosenberg, A. (1983) *Biochemistry 22*, 910–917.
Griffey, R. H., Redfield, A. G., Loomis, R. E., & Dalquist, F. W. (1985) *Biochemistry 24*, 817–822.
Hagen, D. S., Weiner, J. H., & Sykes, B. D. (1978) *Biochemistry 17*, 3860–3866.
Henry, G. D., & Sykes, B. D. (1987) *Bull. Can. Biochem. Soc. 24*, 21–26.
Henry, G. D., & Sykes, B. D. (1990a) *Biochem. Cell Biol. 68*, 318–329.
Henry, G. D., & Sykes, B. D. (1990b) *J. Mol. Biol. 212*, 11–14.
Henry, G. D., Weiner, J. H., & Sykes, B. D. (1986) *Biochemistry 25*, 590–598.
Henry, G. D., Weiner, J. H., & Sykes, B. D. (1987a) *Biochemistry 26*, 3619–3626.
Henry, G. D., Weiner, J. H., & Sykes, B. D. (1987b) *Biochemistry 26*, 3626–3634.
Hilton, B. D., & Woodward, C. K. (1979) *Biochemistry 18*, 5834–5841.
Hvidt, A., & Nielsen, S. O. (1966) *Adv. Protein Chem. 21*, 287–386.
Jencks, W. P. (1969) in *Catalysis in Chemistry and Enzymology*, McGraw-Hill, New York.
Kainosho, M., & Tsuji, T. (1982) *Biochemistry 21*, 6273–6279.
Kim, P. S., & Baldwin, R. L. (1982) *Biochemistry 21*, 1–5.
Kossiakoff, A. A. (1982) *Nature 296*, 713–721.
Kuwajima, K., & Baldwin, R. L. (1983) *J. Mol. Biol. 169*, 299–322.
Leichtling, B. H., & Klotz, I. M. (1966) *Biochemistry 5*, 4026–4037.
Leighton, P., & Lu, P. (1987) *Biochemistry 26*, 7262–7271.
Leo, G. C., Colnago, L. A., Valentine, K. G., & Opella, S. J. (1987) *Biochemistry 26*, 854–862.
Linderstrom-Lang, K. U. (1955) *Spec. Publ.—Chem. Soc. No. 2*, 1–20.
Linderstrom-Lang, K. U., & Schellman, J. A. (1959) *Enzymes, 2nd Ed. 1*, 443–510.
Makino, S., Woolford, J. L., Tanford, C., & Webster, R. E. (1975) *J. Biol. Chem. 250*, 4327–4332.
McIntosh, L. P., Dahlquist, F. W., & Redfield, A. G. (1987) *J. Biomol. Struct. Dyn. 5*, 21–34.
Menger, F. M., & Doll, D. W. (1984) *J. Am. Chem. Soc. 106*, 1109–1113.
Molday, R. S., Englander, S. W., & Kallen, R. G. (1972) *Biochemistry 11*, 150–158.
Morris, G. A. (1980) *J. Am. Chem. Soc. 102*, 428–429.
Morris, G. A. (1984) *Top. Carbon-13 NMR Spectrosc. 4*, 179–196.
Morris, G. A., & Freeman, R. (1979) *J. Am. Chem. Soc. 101*, 760–762.
Nakashima, Y., & Konigsberg, W. (1974) *J. Mol. Biol. 88*, 598–600.
Nozaki, Y., Chamberlain, B. K., Webster, R. E., & Tanford, C. (1976) *Nature (London) 259*, 335–337.
Nozaki, Y., Reynolds, J. A., & Tanford, C. (1978) *Biochemistry 17*, 1239–1246.
O'Neil, J. D. J., & Sykes, B. D. (1988) *Biochemistry 27*, 2753–2762.
O'Neil, J. D. J., & Sykes, B. D. (1989a) *Biochemistry 28*, 699–707.
O'Neil, J. D. J., & Sykes, B. D. (1989b) *Biochemistry 28*, 6736–6745.
Perrin, C. L., & Lollo, C. P. (1984) *J. Am. Chem. Soc. 106*, 2754–2757.
Qiwen, W., Kline, A. D., & Wuthrich, K. (1987) *Biochemistry 26*, 6488–6493.
Reynolds, J. A., & Tanford, C. (1970) *Proc. Natl. Acad. Sci. U.S.A. 66*, 1002–1007.
Richarz, R., Sehr, P., Wagner, G., & Wuthrich, K. (1979) *J. Mol. Biol. 130*, 19–30.
Roberts & Chachaty, C. (1973) *Phys. Chem. Lett. 22*, 348–351.
Robinson, N. C., & Tanford, C. (1975) *Biochemistry 14*, 369–378.
Roder, H., Wagner, G., & Wüthrich, K. (1985a) *Biochemistry 24*, 7396–7407.
Roder, H., Wagner, G., & Wüthrich, K. (1985b) *Biochemistry 24*, 7407–7411.
Schiksnis, R. A., Bogusky, M. J., Tsang, P., & Opella, S. J. (1987) *Biochemistry 26*, 1373–1381.
Smith, G. M., Yu, L. P., & Domingues, D. J. (1987) *Biochemistry 26*, 2202–2207.
Stockman, B. J., Westler, W. M., Mooberry, E. S., & Markley, J. (1988) *Biochemistry 27*, 136–142.
Torchia, D. A., Sparks, S. W., & Bax, A. (1988) *Biochemistry 27*, 5135–5141.
Tuchsen, E., & Woodward, C. (1985a) *J. Mol. Biol. 185*, 405–419.
Tuchsen, E., & Woodward, C. (1985b) *J. Mol. Biol. 185*, 421–430.
van Wezenbeek, P. M. F. G., Hulsebos, T. J. M., & Schoenmakers, J. G. G. (1980) *Gene 11*, 129–148.
Vasant Kumar, N., & Kallenbach, N. R. (1985) *Biochemistry 24*, 7658–7662.
Wagner, G. (1983) *Q. Rev. Biophys. 16*, 1–57.
Wand, A. J., Roder, H., & Englander, S. W. (1986) *Biochemistry 25*, 1107–1114.
Webster, R. E., & Cashman, T. S. (1988) in *The Single-stranded DNA Phages* (Denhardt, D. T., Dressler, D., & Ray, D., Eds.) pp 557–569, Cold Spring Harbor Laboratory, Cold Spring Harbor, NY.
Wickner, W. (1988) *Biochemistry 27*, 1107–1114.
Wilson, M. L., & Dahlquist, F. W. (1985) *Biochemistry 24*, 1920–1928.
Woodward, C., Simon, I., & Tuchsen, E. (1982) *Mol. Cell. Biochem. 48*, 135–160.
Woolford, J. L., & Webster, R. E. (1975) *J. Biol. Chem. 250*, 4333–4339.
Wuthrich, K., & Wagner, G. (1979) *J. Mol. Biol. 130*, 1–18.
Wuthrich, K., Strop, P., Ebina, S., & Williamson, M. P. (1984) *Biochem. Biophys. Res. Commun. 122*, 1174–1178.